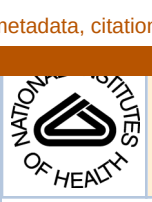

Published in final edited form as:
Adv Healthc Mater. 2013 April ; 2(4): 552–556. doi:10.1002/adhm.201200196.

Image-predicated Sorting of Adherent Cells Using Photopatterned Hydrogels

Dr. J. Kovac,
Department of Electrical Engineering and Computer Science, Massachusetts Institute of Technology, Cambridge, MA 02139 (USA)

Ms. Ylaine Gerardin, and
Department of Systems Biology, Harvard University, Cambridge, MA 02138 (USA)

Prof. J. Voldman
Department of Electrical Engineering and Computer Science, Massachusetts Institute of Technology, Cambridge, MA 02139 (USA)

J. Voldman: voldman@mit.edu

Keywords

genetic screens; hydrogels; microscopy; photopatterning; sorting

Images of cells convey a wealth of information. Researchers routinely use ubiquitous light microscopes to obtain information about cell structure,[1] shape and motility,[2] cell-cell interactions,[3] and protein expression with spatio-temporal resolution.[4] Cell fate prediction using image-based phenotyping is applied to a wide range of cell types, including stem cells. [5, 6] The ability to sort cells following such imaging could offer a number of advantages, such as allowing the direct utilization of cells prospectively identified by imaged phenotypes,[5] and allowing investigation into heterogeneity[7] observed *via* imaging by applying bulk assays to specific cell subpopulations. When developing cell lines, the most visually promising post-transformation clones could be enriched prior to the protracted efforts of dilution cloning. Pooled, barcoded genetic screens, typically limited to phenotypes that can be sorted *via* fluorescence activated cell sorting (FACS)[8] or that alter proliferation,[9] could be expanded to all phenotypes recognizable through microscopy. Unfortunately, facile methods to isolate cells based upon that rich, image-derived information are lacking. FACS offers high throughput,[10] but as it does not *image* cells, it lacks sub-cellular and single-cell temporal resolution, and loses most morphological information because cells are analyzed in suspension. Sorting can be added to microscopy, *via* live-cell adaptations of laser capture microdissection,[11] laser-based killing of undesired cells,[12] or clone picking following imaging. However, these platforms are all prohibitively expensive for individual labs and/or have specific limitations (proprietary culture films,[11] semi-solid media), and thus have not been widely adopted. Here we present a user-friendly, inexpensive method utilizing photopatternable hydrogels to sort cells following imaging. Termed Polymerization-Activated Cell Sorting (PACS), the method utilizes commercially available reagents and hardware found in most biology labs to create an in-lab

Correspondence to: J. Voldman, voldman@mit.edu.

Supporting Information
Supporting Information is available from the Wiley Online Library or from the author.

photolithography system with rapidly reconfigurable photomasking that enables quick sorting of cells following imaging.

Photopatternable hydrogels are formed by shining light onto an aqueous prepolymer solution that crosslinks upon light exposure.[13] By patterning the light with a photomask, tissue engineers have encapsulated cells into specially-shaped hydrogels that act as culture scaffolds;[14] cell viability is ensured by picking judicious operating parameters.[15] While most applications of photopatterned hydrogels seek to preserve encapsulated cells for downstream applications, PACS is the inverse of this traditional use – we use the hydrogel to encapsulate *undesired* cells. In PACS, we print a photomask that shields locations in the culture dish containing desired cells from light exposure and photocrosslink a hydrogel that blankets undesired cells in the unmasked regions (Figure 1a and 1b). We can then release desired cells from the un-gelled regions using an enzymatic cleaving agent (e.g., trypsin) (Figure 1c). To demonstrate selective cell release, we targeted a pair of $mCherry^+$ cells in an $mCherry^+/eGFP^+$ HeLa s3 co-culture, blanketed $eGFP^+$ cells with hydrogel, and released $mCherry^+$ cells with trypsin (Figure 1d). The mask generation process is easily extended to patterning multiple spots in an arbitrary configuration (Figure 1e). Polymerized hydrogels are mostly smooth, with intermittent ridge-like features likely arising from gel stresses (Figure 1e). These ridge-like features do not impact functionality, and polymerized hydrogels are rigid enough to sustain trypsinization and washing procedures.

Prepolymer biocompatibility and fast, inexpensive photomask generation are crucial for PACS. Our prepolymer consists of standard cell culture media, 20% w/v (poly) ethylene glycol diacrylate (PEGDA) (MW 1k), 0.4% w/v UV photoinitiator (PI) (Irgacure 2959), 11,000 U mL^{-1} catalase, and 1.6% v/v methanol. We determined empirically that this prepolymer offered viable cell output with both HeLa s3 cells and MCF7 cells and formed mechanically robust, crisply patterned hydrogels. Briefly, we tested a range of typically-used photoinitiator/PEGDA 3400 concentrations and UV exposure times; these did not form mechanically robust gels suitable for cell sorting. We then used a WST-1 assay to determine the toxicity of other prepolymer components and solutions (specifically lower-MW PEGDA), and found that 10 min. incubation in a prepolymer of 20% PEGDA 1000, 1.5% PI, and 6.0% methanol yielded metabolism results comparable to a culture media control, suggesting that transient incubation in this prepolymer did not significantly impact metabolism. We then performed trial sorts to confirm gel robustness while using this prepolymer, and concluded that we only needed to use 0.4% PI and a 12-min. UV exposure to form robust gels with viable sorted cells, thus allowing use of a less harsh prepolymer than the prepolymer confirmed to not affect cell metabolism. Additionally. the exposure duration was comparable to the 10 min. incubation in the WST-1 trial. This optimization process suggested that cell viability would not be greatly affected using our technique, and is detailed further in the Supporting Information (Supporting Information, Figure S1, Experimental Details). To generate photomasks, we use a position-encoded stage on the microscope to record locations of desired cells identified through microscopy relative to reference marks drawn onto the dish underside (Figure 1a). A custom-written MatLab program generates a mask image from these locations that we print onto a transparency film using an in-lab, standard, inexpensive inkjet printer. We visually align reference marks on the mask to reference marks on the dish (Supporting Information, Figure S2).

Mask alignment and patterned spot size affect sort purity. We measured (Supporting Information, Figure S3, Experimental Details) that we can align mask spots to within 150 μm of their intended targets ~75% of the time (Figure 1f), indicating that a 300-μm-diameter spot should usually cover a targeted point. Although this tolerance is sufficient for many assays, even tighter alignment could be achieved through mechanical mask alignment. Photomask spot diameters are typically ~10–40 μm larger than their design size, while

photopatterned spots are typically ~100 μm larger than their design diameter (Figure 1g). Hereafter, spot sizes refer to the designed spot size diameter.

We examined the impact of patterned well size on cell release and viability by plating skewed (1000:1) ratios of $mCherry^+$:$eGFP^+$- HeLa s3 cells slightly below confluence and enriching for $eGFP^+$ cells using 500 μm, 375 μm, and 250 μm spot sizes (Table 1). We were able to successfully retrieve and grow (Supporting Information, Figure S4 and S5) cells even from the smallest (250 μm) spots, with recovery and re-plating efficiency increasing from 51% to 83% as spot size increased from 250 μm to 500 μm. These data suggest that spots sizes under 250-μm could be used if alignment were improved. We used a 500-μm spot size for subsequent characterization assays to minimize the impact of alignment error for better comparison across experiments.

In some applications, such as pooled barcoded genetic screens, target cell enrichment and throughput are the figures of merit, while absolute output purity is less important. To this end, we seeded skewed (1000:1) $eGFP^+$ and $mCherry^+$- HeLa s3 co-cultures slightly below confluence and attempted to retrieve all minority cells (Table 1). We performed two rounds of iterative sorting, demonstrating that sorted cells could be re-sorted to achieve arbitrary levels of purity (Figure 2a). After a single round of sorting, we achieved up to 87-fold target cell enrichment and up to 1300-fold total enrichment after two rounds of sorting. On average, ~80% of targeted cells were successfully released and re-plated after each sort. We color-biased skew ratios in both directions (1000:1 $mCherry^+$:$eGFP^+$ and 1000:1 $eGFP^+$:$mCherry^+$) to validate that reported performance was not due to acute toxicity to a particular cell line or widely-asymmetric growth rates (Table 1, Supporting Information, Figure S6). We additionally validated sorting functionality with another cell line by sorting skewed populations of fluorescently distinguishable MCF7 cells (Table 1, Supporting Information, Figure S7).

In other applications, such as enriching visually promising clones prior to dilution cloning, absolute output purity is important. To this end, we seeded skewed (9:1) $eGFP^+$ and $mCherry^+$ HeLa s3 co-cultures in both bias directions at a substantially sub-confluent density, cultured cells for four days into small colonies, and retrieved cells from the minority population (Figure 2b, Supporting Information, Figure S8). We restricted retrieval to colonies that we predicted were retrievable with at least 1 target cell per contaminating background population cell to ensure a minimum output purity of 50%; we achieved output purities of 64% and 79% (Table 1). Output purity can be improved by increasing selection criteria stringency at the expense of reducing the total number of cells retrieved.

Development of clonal image-based reporter cell lines necessitates dilution-cloning transformed cells into multi-well plates, imaging wells for the desired phenotype, and expanding desirable clones. Pre-sorting for proper image-based phenotype prior to dilution cloning would restrict dilution cloning efforts to promising cells, increasing clone yield and quality. To this end, we conducted sorts with HeLa s3 cells that expressed an eGFP-CENP-A fusion protein. CENP-A is a centromere protein, and ideal localization of the reporter would result in a phenotype with bright, granular, nuclear-confined, eGFP speckles, with no diffuse background fluorescence. We first FACS-sorted $eGFP^+$ cells into four output populations defined by narrow sort gates on the GFP channel (Figure 2c). Consistent with the fact that FACS cannot resolve localization, each output of the FACS-sorted population revealed heterogeneity of protein localization, which we qualitatively stratified into three distinct phenotypes (Figure 2d). We used a 375-μm mask spot size to sort cells from a single FACS output into three viable separate cultures purified for phenotype A, B, or C to underscore the ability to select an arbitrary image-based phenotype (Figure 2e). We restricted selection to those cells that we believed we could target at a stringency of two or

more desired cells per undesired cell. All three phenotypes were able to proliferate to confluence in a standard 15-cm culture dish. Importantly, Output 3 in Figure 2e was highly enriched for phenotype C, representing isolation of a useful phenotype for developing a CENP-A reporter line; isolation of the other two phenotypes is shown to demonstrate the versatility of the method.

PACS is an inexpensive, user-friendly technique for viable, image-predicated cell sorting. The method leverages commercially available reagents and equipment already found in many biology labs, eliminating the cost barrier of current commercial systems. PACS can immediately offer substantial enrichment of low-incidence populations as well as high-purity samples. The method opens new opportunities in streamlining image-based reporter line development, application of bulk assays to subpopulations in an image-predicated manner, pooled, image-based genetic screens, and any other application that benefits from isolation of cells phenotyped by microscopy.

Experimental Section

Experimental Details

Image acquisition and analysis—We performed imaging using a computer-controllable inverted fluorescence microscope (Eclipse TiE, Nikon) outfitted with a motorized, position-encoded stage (BioPrecision 2, Ludl), CCD camera (CoolSnap HQ^2, Photometrics) and imaging software (NIS-Elements, Nikon). Prior to sorting, we manually inspected the dish for target cells and recorded corresponding images and target cell locations. After sorting, we automatically scanned and recorded composite images of entire wells containing sorted cells. All imaging steps used calcium- and magnesium-containing PBS as the imaging medium. We manually counted populations of sorted red and green cells in recorded images to quantify performance. Image processing techniques used for some images are described in Supporting Information, Experimental Details.

Sorting process equipment and materials—We plated all cells on 40-mm diameter coverslip-bottomed culture dishes (Electron Microscopy Sciences) prior to sorting. Cell ratios and concentrations at seeding were determined using a Z2 Coulter Counter (Becton Dickinson). We wrote MatLab software to generate mask image files. We used an inkjet printer (Hewlett Packard 6540) with cartridges HP 96 and HP 97 to print masks onto copier transparencies (Office Depot 753–631). Exposure system components included an X-Cite 120 fluorescence light source, liquid-core light guide, Zeiss collimating assembly (EXFO Life Sciences), mirror switcher (447230, Zeiss), UG1 filter glass (Thorlabs), and a machined metal baseplate with an ~ 5-cm-diameter aperture that could interface with standard optomechanics. When connected as shown in Supporting Information, Figure S2, beam intensity was ~5–10 mW cm^{-2} (approximate variation over bulb lifetime, centered at 365 nm) at a beam waist of ~ 5-cm-diameter.

Sorting procedure—After printing the corresponding mask and mounting the mask to the mask holder, we aspirated culture media from the culture dish and replaced it with prepolymer. After aligning the dish to the mask, we used a 12 min. exposure for gel crosslinking. Following crosslinking, we aspirated excess prepolymer and rinsed the hydrogel once in calcium- and magnesium-free phosphate buffered saline (PBS) before releasing cells with 0.25% trypsin (Gibco). Following release, we quenched cell-containing trypsin 1:3 with standard culture media and centrifuged the suspension for 5 min. at 200 relative centrifugal force (rcf). We then aspirated the supernatant, washed the cells in standard culture media (10 mL), and centrifuged the suspension for 5 min. at 200 rcf. We then aspirated the supernatant and re-suspended sorted cells in a single well of a 48-well plate.

Cell sorting experiments—Cell seeding densities for 1000:1 ratio experiments with HeLa s3 cells, 9:1 ratio experiments with HeLa s3 cells, and 20:1 ratio experiments with MCF7 cells, were 1.5e5, 6.4e3, and 1.0e4 cells/dish, respectively. Pre-sort culture periods were ~ one day for the 1000:1 experiments, ~ four days for 9:1 experiments, and ~ three days for 20:1 experiments. In all sorts, we imaged the sorted output in single wells of a 48-well plate ~ one day after sorting. For two-stage sorts, we re-plated sorted cells from the first stage into a fresh 40-mm-diameter dish three days after the first round sorting and sorted these cells after ~ three days of culture into single wells of a 48-well plate.

For eGFP-CENPA fusion reporter line sorts, we first sorted $eGFP^+$ cells into four separate outputs gated on relative fluorescence intensity using a DaKo Mo Flo 3 flow cytometer. We plated cells from the “R3” output of the FACS sort (defined in Figure 2c) at 6.4e3 cells/dish into three separate dishes. We cultured cells for five days prior to sorting out one of the target phenotypes from each of the three seeded dishes into separate 48-well plate wells. We cultured output cells in media conditioned by the pre-sort population; details are described in Supporting Information, Experimental Detail.

We discuss cell lines and culture, prepolymer mixing, image processing, and other experimental details in Supporting Information, Experimental Detail.

Supplementary Material

Refer to Web version on PubMed Central for supplementary material.

Acknowledgments

This research was supported by the National Institutes of Health (RR19652) and the Singapore-MIT Alliance. J.R.K. was supported by a National Science Foundation graduate research fellowship and a Department of Defense graduate fellowship. We thank Nicholas Kuperwasser (HMS), Alexander Loewer (HMS), and Sara Thiebaud (HMS) for constructing HeLa s3, $mCherry^+$ MCF7, and $eYFP^+$ MCF7 cell lines, respectively. We thank Alice Chen (MIT) and Daniel Pregibon (MIT) for fruitful discussions. Supporting Information is available online from Wiley InterScience or from the author.

References

1. Maniotis AJ, Chen CS, Ingber DE. Proceedings of the National Academy of Sciences of the United States of America. 1997; 94:849. [PubMed: 9023345]
2. Keren K, Pincus Z, Allen GM, Barnhart EL, Marriott G, Mogilner A, Theriot JA. Nature. 2008; 453:475. [PubMed: 18497816]
3. Dakin K, Zhao YR, Li WH. Nature Methods. 2005; 2:55. [PubMed: 15782161]
4. Geva-Zatorsky N, Rosenfeld N, Itzkovitz S, Milo R, Sigal A, Dekel E, Yarnitzky T, Liron Y, Polak P, Lahav G, Alon U. Molecular Systems Biology. 2006
5. Cohen AR, Gomes FLAF, Roysam B, Cayouette M. Nature Methods. 2010; 7:213. [PubMed: 20139969]
6. Chan EM, Ratanasirintrawoot S, Park IH, Manos PD, Loh YH, Huo HG, Miller JD, Hartung O, Rho J, Ince TA, Daley GQ, Schlaeger TM. Nature Biotechnology. 2009; 27:1033.
7. Huang S. Development. 2009; 136:3853. [PubMed: 19906852]
8. Guryanova OA, Makhanov M, Chenchik AA, Chumakov PM, Frolova EI. Molecular Biology. 2006; 40:396. [PubMed: 19777129]
9. Mullenders J, Fabius AWM, Madiredjo M, Bernards R, Beijersbergen RL. Plos One. 2009:4.
10. Ashcroft RG, Lopez PA. J Immunol Methods. 2000; 243:13. [PubMed: 10986403]
11. Horneffer V, Linz N, Vogel A. Journal of Biomedical Optics. 2007:12.
12. Koller MR, Hanania EG, Stevens J, Eisfeld TM, Sasaki GC, Fieck A, Palsson BO. Cytometry Part A. 2004; 61A:153.

13. Liu VA, Bhatia SN. Biomed Microdevices. 2002; 4:257.
14. Khademhosseini A, Eng G, Yeh J, Fukuda J, Blumling J, Langer R, Burdick JA. Journal of Biomedical Materials Research Part A. 2006; 79A:522. [PubMed: 16788972]
15. Williams CG, Malik AN, Kim TK, Manson PN, Elisseeff JH. Biomaterials. 2005; 26:1211. [PubMed: 15475050]
16. Shaner NC, Campbell RE, Steinbach PA, Giepmans BNG, Palmer AE, Tsien RY. Nature Biotechnology. 2004; 22:1567.
17. Jullien D, Vagnarelli P, Earnshaw WC, Adachi Y. Journal of Cell Science. 2002; 115:71. [PubMed: 11801725]
18. Batchelor E, Mock CS, Bhan I, Loewer A, Lahav G. Molecular Cell. 2008; 30:277. [PubMed: 18471974]
19. Pagoria D, Lee A, Geurtsen W. Biomaterials. 2005; 26:4091. [PubMed: 15664636]
20. Ciba® IRGACURE® 2959 datasheet. Jun. 2012 http://www.xtgchem.cn/upload/20110629045632.PDF
21. Layson Bio. Jun. 2012 web site, http://laysanbio.com/

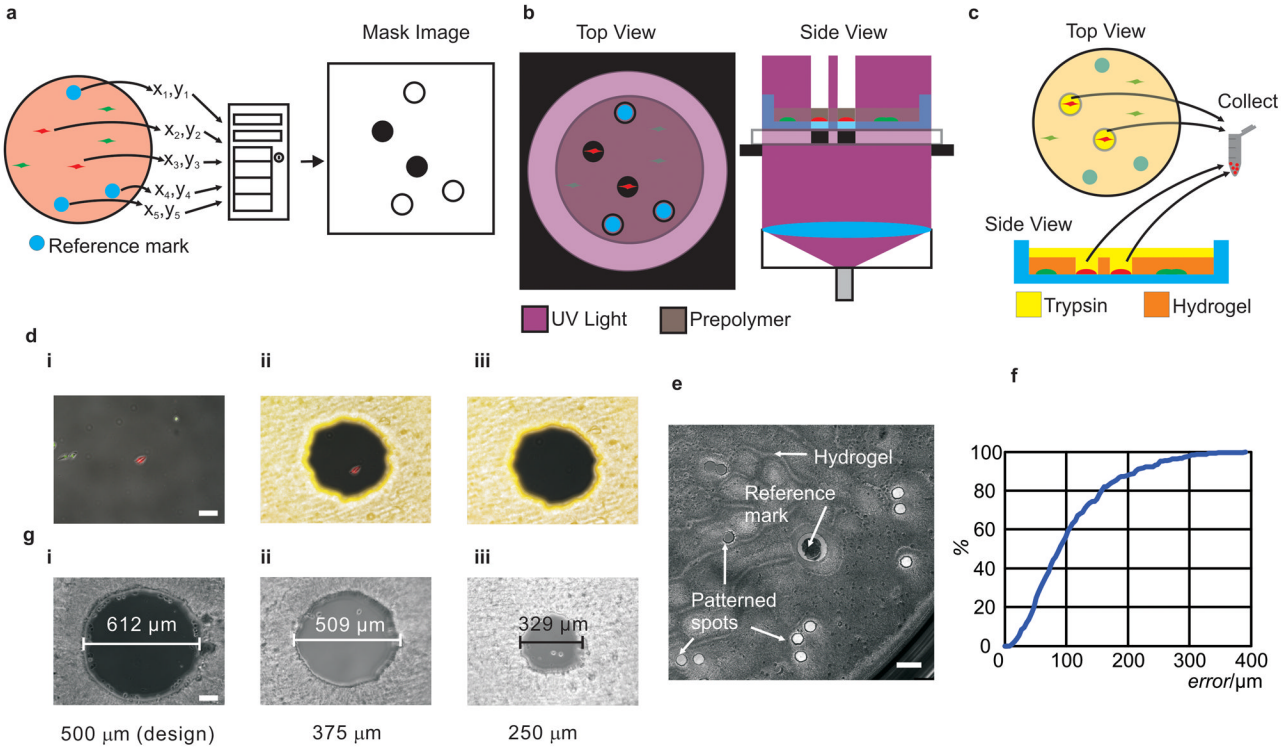

Figure 1.

PACS operation. (a) Based on target cell locations, software generates a photomask image and prints a transparency mask with black spots corresponding to target cell locations. (b) The aligned transparency patterns UV light, allowing prepolymer crosslinking except in masked regions. (c) Enzymatic release and retrieval of cells in un-crosslinked regions. (d) Demonstration of (i) targeting an mCherry$^+$ cell in a mixed mCherry$^+$/eGFP$^+$ population, (ii) forming a hydrogel well around the mCherry$^+$ cell, and (iii) releasing the mCherry$^+$ cell with trypsin; scale bar is 100 μm. (e) Large-area image of a hydrogel; scale bar is 1 mm. Image is a tiled composite of fields. (f) Percentage of spots whose alignment error was less than the indicated amount. (g) Patterned hydrogel spot diameter vs. design diameter; scale bar is 100 μm.

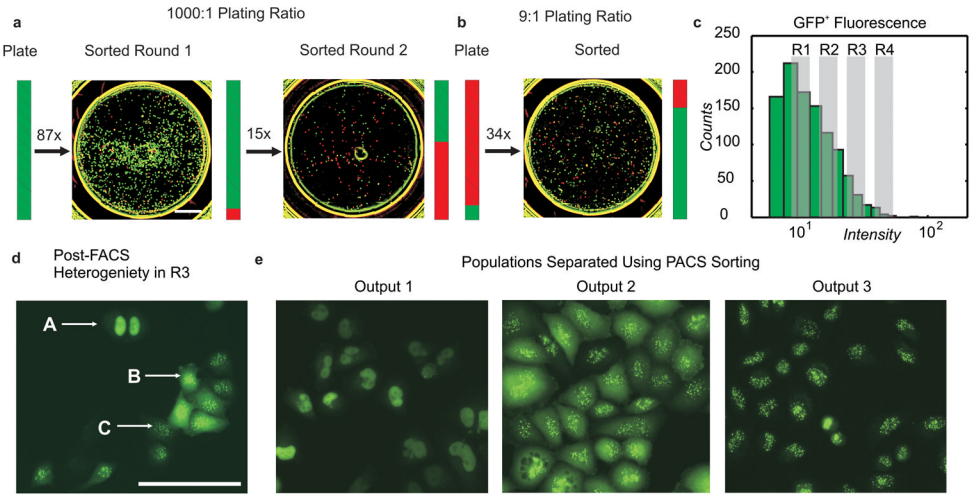

Figure 2.

Sorting experiments. (a) Two-round sort emphasizing output enrichment. Sorted output cells shown over two rounds of sorting, plated at a 1000:1 $eGFP^+$:$mCherry^+$ ratio prior to sorting. We achieved 87-fold enrichment of $mCherry^+$ cells after one round, and an additional 15-fold enrichment after two rounds. Bars indicate relative population sizes at each stage; hatched color indicates undesired cell population; scale bar is 2 mm. (b) One-round sorting process emphasizing output purity. Sorted output cells initially plated at a 9:1 $mCherry^+$:$eGFP^+$ ratio at low density. We achieved 34-fold enrichment and 79% output purity of $eGFP^+$ cells. (c) FACS histogram of eGFP-CENP-A fusion reporter line, showing locations of four output gates (R1-R4); generation of plot is discussed in Supporting Information, Experimental Details. (d) Image of eGFP localization heterogeneity in R3 FACS output; scale bar is 100 μm. (e) Localization phenotypes sorted *via* PACS. Images in (a), (b), (d), and (e) are sections of larger tiled composites of imaged fields. Fluorescence signals from cells in (a) and (b) were dilated and additionally processed as described in Supporting Information, Experimental Details to maximize cell visibility; images without this dilation step are shown in Supporting Information, Figure S6 and S8.

Table 1

Performance quantification from spot size comparison. Enrichment is defined as $(M/B)_{final}/(M/B)_{initial}$, where M is the size of the target population, B is the size of the undesired population, and *initial* and *final* refer to evaluation before and after sorting, respectively. Output purity is the percentage of target cells in the output. Transfer efficiency is the number of target cells found in the output well the day after sorting divided by the number of attempted target cell retrievals, multiplied by 100%.

Spot Size Comparison				
Spot Diameter [μm]	**Output Ratio (R:G)**	**Fold- Enrichment**	**Output Purity [%]**	**Transfer Efficiency [%]**
500	67:1	15	1.5	83
375	24:1	42	4.1	75
250	17:1	60	5.7	51

HeLa s3 Multi-stage Sorts				
Plating Ratio (R:G)	**Output Ratio (R:G)**	**Fold- Enrichment**	**Output Purity [%]**	**Transfer Efficiency [%]**
1000:1 Round 1	57:1	18	1.7	82
1000:1 Round 2	1.7:1	590 (overall)	37	89
1:1000 Round 1	1:12	87	8.0	97
1:1000 Round 2	1.3:1	1300 (overall)	56	56

HeLa s3 Single-stage Sorts				
Plating Ratio (R:G)	**Output Ratio (R:G)**	**Fold- Enrichment**	**Output Purity [%]**	**Transfer Efficiency [%]**
9:1	1:3.8	34	79	52
1:9	1.8:1	16	64	69

MCF7 Single-stage Sorts				
Plating Ratio (R:G)	**Output Ratio (R:G)**	**Fold- Enrichment**	**Output Purity [%]**	**Transfer Efficiency [%]**
20:1	1:1.2	24	55	79
1:20	1:1.8	11	36	62